HHS Public Access

Author manuscript

Osteoarthritis Cartilage. Author manuscript; available in PMC 2022 April 01.

Published in final edited form as:

Osteoarthritis Cartilage. 2021 April ; 29(4): 547–557. doi:10.1016/j.joca.2021.01.005.

ADAMTS5 Is Required For Normal Trabeculated Bone Development In The Mandibular Condyle

Alexandra W. Rogers-DeCotes[1], **Sarah C. Porto**[2], **Loren E. Dupuis**[3], **Christine B. Kern**[*,1]

[1]Department of Regenerative Medicine and Cell Biology, Medical University of South Carolina Charleston, SC 29525.

[2]Department of Health and Human Performance, College of Charleston, Charleston, SC 29424.

[3]Medical University of South Carolina, Division of Cardiothoracic Surgery, Charleston, SC 29525.

Abstract

Objective: Determine the role of the extracellular matrix protease ADAMTS5 in development of the trabeculated bone of the mandibular condyle.

Methods: The mandibular condyles of wild type and mice deficient in the protease ADAMTS5 were examined for histopathology with Safranin O staining. Microcomputed tomography was performed to analyze the developing bone of the mandibular condyle. RNAscope and immunohistochemistry were utilized to investigate cell type and extracellular matrix expression.

Results: Mice deficient in *Adamts5*, (*Adamts5*$^{tm1Dgen/J}$) exhibit an increase in trabecular separation (n=37 wild type; n= 27: $P<0.0001$) and reduction of trabecular thickness $P=0.0116$ and bone volume fraction $P=0.0869$ in the mandibular condylar head compared to wild type littermates. The altered bone parameters were more pronounced in male *Adamts5*$^{-/-}$ mice compared to female *Adamts5*$^{-/-}$ mice (TbSp; $P=0.03$). *Adamts5* was co-expressed with versican and Gli1 in mesenchymal, stem-like cells in the transition zone where the trabeculated bone is adjacent to mature hypertrophic chondrocytes. Loss of *Adamts5* caused a reduction of *Bglap* expressing osteoblasts throughout mandibular condylar development and in young adult mice. The protease *Mmp13*, that is involved in mineralization and is expressed by hypertrophic chondrocytes and osteoblasts, was reduced in the mandibular condyle of *Adamts5* deficient mice.

Conclusion: This is the first report of a novel and critical role for *Adamts5* in bone formation within the mandibular condyle of the temporomandibular joint. These data indicate *Adamts5*

[*]Corresponding author: kernc@musc.edu.

1.9.8**Contributions**: AWR was involved in the design and acquisition and analysis of data, performed statistical studies, drafting of the article and approved the final submitted version. SCP facilitated the conception of the study, acquired data, performed statistical studies, revised a manuscript draft and approved the final submission. LED was involved in the design of the experiments, generated the models and provided intellectual content and approved the final version for submission. CBK was involved in the conception of the study, interpretation of the data, writing the manuscript and funding of the study as well as approval of the final submission.

1.9.10**Competing interest statement:** The authors do not have any competing interests to declare.

may be required in the transdifferentiation of hypertrophic chondrocytes to osteoblasts during trabecular bone formation in development of the mandibular condyle.

Keywords

Mandibular condyle; Temporomandibular Joint (TMJ); ADAMTS; Extracellular matrix; bone

1.9.3 Introduction:

Temporomandibular joint (TMJ) disorders affect approximately 10 million Americans each year, yet the TMJ is a relatively understudied joint [1–3]. The mandibular condyle of the TMJ is comprised of fibrocartilage that is arranged in a zonal architecture of cells at different stages of chondrogenic development with each layer containing a distinct and specialized extracellular matrix (ECM). Mature hypertrophic chondrocytes comprise the deepest layer of the mandibular condylar cartilage (MCC) adjacent to the subchondral bone that forms during postnatal development [4]. While cartilage and bone formation [5] are interconnected in the mandibular condyle, the molecular mechanisms involved remain poorly understood.

The dogma states that hypertrophic chondrocytes undergo programed cell death, as the surrounding matrix is ossified while mesenchymal precursors of osteoblasts migrate from the bone marrow and periosteum [5] to synthesize the bone matrix. Studies in mice have shown that mechanical load impacts endochondral ossification and is likely a key factor in the dramatic changes of the mandibular condyle after birth due to nursing and then adaptation to a hard-pellet diet [6]. The coordinated processes of chondrogenesis, cell proliferation, apoptosis and bone formation are all essential in the adaptability and health of the TMJ.

There is an additional mechanism of endochondral bone formation where hypertrophic chondrocytes transdifferentiate into bone producing cells (defined as osteoblasts and osteocytes). Although first noted in organ cultures in the 1930’s, there have been many subsequent reports that validate a role for the transdifferentiation of hypertrophic chondrocytes into bone cells [7]. Molecular tools that allow lineage tracing have conclusively shown that chondrocytes transform directly into bone matrix secreting cells. In fact in the transition zone of the mandibular condyle the majority of bone cells are derived from hypertrophic chondrocytes [8] [9] [10] while deeper in the condylar neck a greater percentage of osteoblasts are derived from undifferentiated mesenchymal cells contributed by the bone marrow [11].

In active regions of bone deposition and remodeling, there are high levels of ECM matrix metalloproteases [12] [13]. MMP9 is expressed by osteoclasts, while MMP13 is expressed by both hypertrophic chondrocytes and osteoblasts. Here we investigate a potential role for A Disintegrin And Metalloproteinase with ThromboSpondin Motifs 5 (ADAMTS5) protease in the formation of trabecular bone in the mandibular condyle. Previous expression studies of *Adamts5* using a lacZ knock-in reporter strain, demonstrated that *Adamts5* is expressed in bone lining cells [14] however, the cell-type or role for ADAMTS5 in bone development and the mandibular condyle has not been investigated. In mice deficient in ADAMTS5 knee

joints have a significantly thinner subchondral plate and less epiphyseal trabecular bone compared to wild type, however they are protected from cartilage damage after ligament transection in contrast to wild type that had significant damage [15].

Recently we determined that the ECM protease ADAMTS5 was required for normal mandibular condylar cartilage development. Mice deficient in the ADAMTS5 protease exhibit a lack of zonal organization of chondrocytes and ECM. In addition, ADAMTS5 deficient mice develop more severe osteoarthritic-like changes in their TMJ fibrocartilage by six months of age compared to wild type littermates. Additional consequences of ADAMTS5 deficiency in the TMJ is the accumulation of its cartilage proteoglycan substrate aggrecan (Acan), and reduction of mature hypertrophic chondrocytes [16]. Here we investigated the hypothesis that *Adamts5* is critical for trabecular bone formation during mandibular condylar development of the TMJ.

1.9.4 Materials and Methods:

Generation of Adamts5$^{-/-}$ Mice:

Animal protocols were approved by the Medical University of South Carolina Institutional Animal Care and Use Committee (IACUC). The standard twelve-hour light cycle was diurnal. There was unlimited access to food and water, supplied via reverse osmosis system and dispensed into Lab Product rodent bottles/sippers. Purina Lab Diet 5V75 (standard diet) and 5VM5 (breeder diet) was utilized with unlimited supply and access. The bedding source is autoclaved corn cob (Bed'o'Cobs) supplied by Anderson Lab Bedding. The *Adamts5*$^{-/-}$ mice used in this study were the *Adamts5*$^{tm1Dgen/J}$ (The Jackson Laboratory, Bar Harbor, ME) that were bred into C57BL/6J (> 20 generations) and maintained as previously described [17, 18]. Genotyping of *Adamts5* mice was performed using PCR as previously published [18]. The *Adamts5*$^{-/-}$ mice used in this study do not exhibit any pain or distress. Euthanasia approved protocols for age endpoint for analysis.

Tissue Collection, and Histomorphometrics

Adamts5$^{+/+}$ (wild type) and *Adamts5*$^{-/-}$ mouse heads were bisected at postnatal day 7 (P7), postnatal day 14/15 (P14/15), postnatal day 21 (P21) and 2 months of age. The left side of the head was fixed in 4% paraformaldehyde, decalcified in 0.5 M EDTA, pH 8.0 for 1 week (P7), 2–3 weeks (P14/P15), or 4–5 weeks (P21 and 2 months) and processed for microcomputed tomography, histology, Tartrate-Resistant Acid Phosphatase (TRAP) staining and immunohistochemistry (IHC). Tissue was embedded for sectioning of the mandibular condyles in the saggital plane at 8 micrometers (μm) for Safranin O/Fast Green staining and 5 μm for RNAscope™. Safranin O/Fast Green staining was utilized for all histomorphometric analysis. The right side of the head was fixed in 4% paraformaldehyde for 42–44 hours, decalcified in 0.5 M EDTA, pH 8.0 as described above and processed for RNAscope™.

Microcomputed tomography:

Mineralized cartilage and subchondral bone were analyzed using microcomputed tomography (SCANCO Medical *ex vivo* uCT40 AG, Brüttisellen, Switzerland). The 4%

paraformaldehyde fixed samples were individually scanned in 70% Ethanol in a 9 mm holder. Serial tomographic projections were acquired at 70 kV and 114μA, with a voxel size of 6μm and 1000 projections per rotation collected at 300000 μs. The DICOM images were transferred, segmented and reconstructed using the AnalyzeDirect/AnalyzePro software (Overland Park, KS). Total bone volume (TV (mm^3)), bone volume (BV (mm^3)), bone volume fraction (BV/TV (%)), trabecular thickness (TbTh (mm)) and trabecular separation (TbSp (mm)) were determined. The microcomputed tomography was performed based on a randomly assigned number that blinded the operator of the scanner and subsequent analysis performed by the AnalyzeDirect/AnalyzePro software (Overland Park, KS).

Statistical Analysis:

In graphs, each symbol represents data from a mandibular condyle from a single mouse (n=1). The longest horizontal bar represents the mean value of the graphed measurements. In the case of the bone marrow infiltration measurements, there were significant differences of variances between groups, therefore the Mann-Whitney nonparametric test was used. Student's t-test was used to analyze pooled male/female wild type and *Adamts5*$^{-/-}$ μCT data, and one-way ANOVA was utilized for analysis of the male/female wild type and *Adamts5*$^{-/-}$ condylar heads. The paired t-test was used for *Bglap* mRNA. Student's t-test was performed to compare the following expression analyses between *Adamts5*$^{+/+}$ and *Adamts5*$^{-/-}$: *Mmp13*, Vcan and Gli1 developmental and 2mo comparisons, *Ctsk*, TRAP and *Mmp9*. GraphPad Prism 8 was utilized for statistical analysis and graphing. For the μCT data the longest horizontal bar represents the mean value of the graphed measurements, with the shorter bars representing the standard deviation. The Confidence Intervals, (95% CI) are included. The animal numbers were assigned randomly prior to genotyping, this served to blind the investigators at every stage of the study, until the grouping for statistical analysis. We performed het X het matings to obtain all of the wild type and *Adamts5*$^{-/-}$ used in this study; for example that required eleven different litters used to obtain enough animals for the 2 mo Safranin O staining used to evaluate the bone marrow infiltration (Fig. 2). Littermates with the het X het matings are treated as independent. The quantitative analyses using histological sections, was performed blinded to genotype and scored by two different lab members, and the resulting values were averaged.

1.9.5 Results:

The interface of hypertrophic chondrocytes and trabeculated bone is altered in the mandibular condyle of *Adamts5*$^{-/-}$ mice and results in an increase in bone marrow in the condylar head and neck.

During postnatal development of the mandibular condyle, trabeculated bone is generated at the interface, i.e. transition zone, with hypertrophic chondrocytes. Since *Adamts5*$^{-/-}$ mice exhibit a reduction in hypertrophic chondrocytes in the MCC [16], we investigated the hypothesis that the trabecular bone may be impacted in the mandibular condyle due to the interconnection of hypertrophic chondrocytes and bone formation [5, 9–11, 19]. Histopathology utilizing Safranin O stained sections of postnatal day (P7) and P15 mandibular condyles (n=5, each age, genotype) revealed mesenchymal cells bounded by

cartilage matrix (Fig. 1D, H; yellow arrows) compared to the wild type transition zone (Fig. 1C, G) where the mesenchymal-like cells were no longer encapsulated in cartilage matrix.

In addition, the bone marrow, denoted as dark purple stained round cells, encroached farther into the mandibular condylar head of *Adamts5*$^{-/-}$ mice (Fig. 1 F, J, L; green arrows) compared to wild type littermates (Fig. 1E, I, K). In sections from 2 month-old (mo) mice the distance from the deepest hypertrophic chondrocytes in the MCC to bone marrow was quantified (Fig. 1, green bars); the distribution of bone marrow was different in 2mo *Adamts5*$^{-/-}$ mice (n=16) compared to wild type (n=19, P<0.0001, Mann-Whitney U, 142; 95% CI −661.1 to −245.6, R= 0.2819) (Fig. 1M). The bone marrow increase was localized to the enlarged trabecular spacing in the condylar head of *Adamts5*$^{-/-}$ mice (Fig. 1E, F; green arrows).

To determine if the reduction in trabeculated bone in the *Adamts5*$^{-/-}$ mandibular condyle may be a primary result of *Adamts5* deficiency, the expression of *Adamts5* was investigated in regions of bone formation during mandibular condylar development (Fig. 3). *Adamts5* was present in the trabeculated bone, with the highest expression at the cartilage-bone interface (Fig. 1N–P; brown). As development progressed there was an apparent reduction in *Adamts5* positive cells in the cartilage-bone interface from P7 (Fig. 1N, O) to adult (Fig. 1P). Therefore the prominent developmental expression of *Adamts5* in the transition zone may contribute to the increase in trabecular spacing in the *Adamts5*$^{-/-}$ mandibular condyle.

We propose that the expression of ADAMTS5 in the mesenchymal cells of the transition zone is required to cleave its cartilage substrate, Acan that is a key component of the pericellular matrix of hypertrophic chondrocytes. The mesenchymal cells of the *Adamts5*$^{-/-}$ mice appear trapped within the Acan-rich hypertrophic cell matrix and are unable to populate the trabecular spaces of the growing mandibular condyle. Subsequently, without mesenchymal-like cells adhering to the trabeculae in the transition zone, bone marrow infiltrates the enlarging trabecular space within the *Adamts5*$^{-/-}$ mandibular condyle. The ADAMTS5 deficient mandibular condyle exhibited changes in the transition zone during development; in young adult *Adamts5*$^{-/-}$ mice, this resulted in an increased amount of trabecular spacing with infiltration of bone marrow closer to the transition zone compared to wild types.

Microcomputed tomography reveals significant adverse changes to the trabeculated bone of the mandibular condyle in Adamts5$^{-/-}$ mice.

To determine if the histopathology of the mandibular condyle was indicative of altered bone composition in the *Adamts5*$^{-/-}$ mice, microcomputed tomography (μCT) was performed on two-month old wild type (n=37) and *Adamts5*$^{-/-}$ (n=27) mandibular condyles. Three-dimensional (3D) reconstruction of the μCT data from a representative wild type (Fig. 2A) and *Adamts5*$^{-/-}$ mandibular condyle (Fig. 2B) are shown. The red box (Fig. 2a) denotes the region of quantification in the μCT analysis. Although the 3D images of wild type and *Adamts5*$^{-/-}$ mandibular condyles varied slightly, there were no consistent gross morphological differences between genotypes in the 3D images generated from μCT reconstructions. However, the μCT data revealed differences in the trabeculated bone of the *Adamts5*$^{-/-}$ mandibular condyle. There was an increase in Total Volume (TV, Fig. 2C)

in *Adamts5*$^{-/-}$ mandibular condyle compared to wild type (*P*=0.0053; 95% CI 0.01546 to 0.08456). The Bone Volume (BV, Fig. 2D) was not different between groups (*P*=0.0869; 95% CI - 0.003168 to 0.04561). The bone volume fraction, Bone Volume/Total Volume (or bone volume density, BV/TV) was reduced in the *Adamts5*$^{-/-}$ mandibular condyles in comparison to wild type (Fig. 2E; *P*<0.0001; 95% CI −12.55 to −4.757). There was also a decrease in the Trabecular Thickness (TbTh, Fig. 2F; *P*=0.0116; 95% CI −0.01066 to −0.001398) and an increase in the Trabecular Separation (TbSp, Fig. 2G; *P*<0.0001; 95% CI 0.006140 to 0.01487) of the Adamts5$^{-/-}$ mandibular condyle. The rather dramatic increase of the TbSp is algins with the increased TV in the *Adamts5*$^{-/-}$ mandibular condyles. These μCT analysis are consistent with the histopathology data (Fig. 1) and indicate a role for ADAMTS5 in trabecular bone development within the mandibular condylar head.

Mandibular condylar μCT analysis was also evaluated by comparing female versus male mice in wild type and *Adamts5*$^{-/-}$ mandibular condyles (wild type female (n=22), *Adamts5*$^{-/-}$ female (n=14), wild type male (n=15) as well as *Adamts5*$^{-/-}$ male (n= 11) mice. There was a significant difference between female and male *Adamts5*$^{-/-}$ mandibular condyles, with young male mice having a greater increase in the TbSp compared to female *Adamts5*$^{-/-}$ mice (Fig. 2L; *P*=0.03; 95% CI 0.0007185 to 0.01668). Comparison of the male and female wild type and *Adamts5*$^{-/-}$ mandibular condyles also indicated that male and female *Adamts5*$^{-/-}$ mandibular condyles were significantly different from the wild type of each sex in TbSp (Fig. 2L; Female- *P*=0.007; 95% CI −0.01615 to - 0.001989: Male- *P*= 0.003; 95% CI −0.01882 to −0.003119) and BV/TV (Fig. 2M; Female- *P*=0.11; 95% CI −0.9035 to 12.27: Male- *P*<0.0001, 95% CI 4.190 to 18.79). The μCT values and the statistical analysis of each group including *P* values and CI 95% is shown in Supplemental Table 1. Collectively, these μCT data revealed that there were significant and detrimental differences in bone parameters in the *Adamts5*$^{-/-}$ mandibular condyles and that the male *Adamts5*$^{-/-}$ mice exhibited a more severe trabecular bone phenotype than *Adamts5*$^{-/-}$ female mice at 2mo.

Adamts5 is expressed by mesenchymal stem like cells in the developing trabeculated bone of the mandibular condyle.

Double-label RNAscope™ was used to determine the cell-type(s) expressing *Adamts5* in trabeculated bone during mandibular condylar development and in the young adult. Co-localization of mRNA from *Adamts5* and Bone Gamma-Carboxyglutamate Protein (*Bglap*, i.e. Osteocalcin), a marker of osteoblasts, was performed (Fig. 3D–I). At P7, there was very little *Bglap* expression in the cartilage-bone interface (Fig. 3D; black box and 3G; blue-green). The expression of *Adamts5* (Fig. 3G; red) did not overlap with *Bglap* expressing cells (Fig. 3G; blue-green). As development progressed, the number of cells expressing *Bglap*, as well as the relative amount of *Bglap* transcripts increased (Fig. 3E, F, H, I; blue-green). Overall there were relatively few cells that co-expressed both *Bglap* and *Adamts5* (Fig. 3H; open arrow). In the adult, cells at the cartilage-bone interface expressed *Adamts5* (Fig. 3I: black arrows) but the expression did not overlap with *Bglap* positive cells (Fig. 3I; yellow arrow). The lack of co-expression of *Bglap* and *Adamts5* in the mandibular condyles indicate that mature osteoblasts do not express the ECM protease *Adamts5*.

Next dual RNAscope™ was performed with *Adamts5* and the osteoclast marker, Cathepsin K (*Ctsk*) in mandibular condyles from P7, P15 and 2mo, young adult mice. Notably, RNAscope™ of *Ctsk* revealed two populations of cells in the trabeculated bone, low expressing (Fig. 3J, blue arrow) and high expressing (Fig. 3F; green arrow). The high expressing *Ctsk* cells, densely covered with *Ctsk* RNAscope™ probe, depict osteoclasts. However, the *Adamts5* expression overlapped with cells expressing low levels of *Ctsk* (Fig. 3K, L; open arrows) indicating that *Adamts5* was not expressed in differentiated osteoclasts of the mandibular condyle.

Adamts5 did not colocalize with either differentiated osteoblast or osteoclast cell markers, and was more highly expressed in mesenchymal, stem-like cells; this indicated that *Adamts5* may be involved in the transdifferentiation of hypertrophic cells in this region [8] [9] [10] [11]. Dual- RNAscope™ was performed with *Adamts5* and either *Vcan* or *Gli1*, markers of undifferentiated mesenchymal cells and stem cells respectively [20, 21] [22]. At P7 there was significant overlap of *Adamts5* with *Vcan* (Fig. 3M; black arrows), while there was colocalization of *Adamts5* with *Gil1* at P15, and P21 (Fig. 3N, O; black arrows). Collectively these data reveal that *Adamts5* was expressed in the cartilage-bone interface during mandibular condylar development and co-localized with markers of undifferentiated mesenchymal cells that have been shown to differentiate into bone producing cells [8] [9] [10] [11].

To determine if the loss of ADAMTS5 resulted in fewer mesenchymal stem-like progenitors in the transition zone of the mandibular condyle, the relative expression of *Vcan* and *Gli1* was evaluated in wild type and *Adamts5*$^{-/-}$ mice. The expression of *Vcan* at P7 and 2mo was similar in each genotype (Supplemental Figure 1A–J, S). The expression of *Gli1* was evaluated at P15, P21 and 2mo; while there was a trend of reduced *Gli1* in the *Adamts5*$^{-/-}$ mice the *P* value was not below $P < 0.05$ ($P = 0.1269$; 95%CI −92.87 to 14.87; Supplemental Figure 1K–R, T). However, Gli1 is also a marker of bone progenitor cells [23], so even a slight reduction of Gli1 during development may impact bone formation in the mandibular condyle of the *Adamts5*$^{-/-}$ mice and contribute to the bone phenotype.

There is a reduction of osteoblasts in the developing mandibular condyle of *Adamts5*$^{-/-}$ mice.

To determine if loss of *Adamts5* disrupted osteoblast differentiation in the transition zone of the mandibular condyle, *Bglap* expression was evaluated by RNAscope™ at postnatal day 7, 14, 15, 21 and 2mo in wild type and *Adamts5*$^{-/-}$ mandibular condyles (Fig. 4A–H; blue-green; black arrows). At each developmental stage examined, there was a reduction in *Bglap* expression in the *Adamts5*$^{-/-}$ subchondral bone compared to wild type and ranged from a 17-fold at P7 to 1.4-fold in 2mo young adults (*P* = 0.0475, 95%CI 0.07840 to 0.9773; Fig. 4M, n=5 wildtype; n=5 *Adamts5*$^{-/-}$). These data are consistent with a reduced number of osteoblasts in the developing mandibular condyle of *Adamts5*$^{-/-}$ mice and may contribute to the significant reduction in BV/TV and TbTh as well as the increase in TbSp that were revealed by μCT.

Expression of *Mmp13*, an ECM protease essential for calcification and expressed by osteoblasts and hypertrophic chondrocytes, was also decreased in the mandibular condyle

of *Adamts5*$^{-/-}$ mice at P7 (P = 0.0173, 95%CI −16.68 to −2.373; Fig. 4I, J, N; n=4 each genotype) and 2mo (P = 0.0313, 95%CI −2.314 to −0.1828; Fig. K, L, N; n=3, each genotype). These data indicate that *Adamts5* may be required for the formation of osteoblasts in the trabeculated bone of the mandibular condyle, and the reduction of *Mmp13* expression in osteoblasts in the *Adamts5*$^{-/-}$ mandibular condyles may contribute to altered bone remodeling.

We also investigated the number of osteoclasts in the wild type and in the *Adamts5*$^{-/-}$ mandibular condyles using the osteoclast marker Ctsk (RNAscope), TRAP staining and MMP9 (RNAscope). We did not observe a significant difference in expression of the osteoclast marker *Ctsk* in the P7, P15 and 2mo *Adamts5*$^{-/-}$ although there was a trend toward reduced expression in age-matched pairs (P = 0.14, 95%CI 0.2770 to 1.453). However, the number of 2mo TRAP positive osteoclasts were reduced (n=12 wild type; n=13 *Adamts5*$^{-/-}$; P=0.0158; 95% CI −15.33 to =1.759) in the developing *Adamts5*$^{-/-}$ condyles (Supplemental Figure 2).

1.9.6 Discussion:

This study revealed that loss of ADAMTS5 had significant and detrimental consequences to the trabecular bone in the mandibular condyle; the *Adamts5*$^{-/-}$ bone phenotype emerged during postnatal development and correlated with a reduced number of osteoblasts. The schematic in Figure 5 highlights cell transitions that lead to the phenotype of the *Adamts5*$^{-/-}$ bone in the mandibular condyle that are dependent on ADAMTS5. To date, the focus of ADAMTS5 has been on the degradation of cartilage matrix where it proteolytically cleaves Acan, an essential cartilage proteoglycan[24]. These data revealed that Adamts5 is expressed by mesenchymal, stem-like cells within the cartilage-bone interface; cells that have shown to de-differentiate from hypertrophic chondrocytes and become osteoblasts [5, 9–11, 19]. The *Adamts5*$^{-/-}$ TMJ phenotype suggest that ADAMTS5 may be involved in the response to changes in mechanical load and impacts both chondrogenesis[16] and osteogenesis within the mandibular condyle.

Until recently, the accepted dogma of endochondral bone formation stated that hypertrophic chondrocytes undergo widespread apoptosis with most of the bone forming cells deriving from the bone marrow and periosteum. However, recent work revealed that in the mandibular condyle, a majority of subchondral bone is generated by the transdifferentiation of chondrocytes into osteoblasts and/or osteocytes [5, 9–11, 19]; this has also been shown in limb cartilage, albeit to a lesser extent [8] [9] [10]. While the cellular transitions involved in the transformation of hypertrophic chondrocytes into bone-forming cells have not been determined, it is possible that hypertrophic chondrocytes undergo de-differentiation into stem cell- like progenitors, receive cues and subsequently differentiate to osteoblasts and/or osteocytes. *Adamts5* expression is highest in mesenchymal-like cells at the interface of the trabecular bone and MCC; this region also exhibits the greatest percentage (80%) of bone cells that are derived from chondrocytes [11]. The lineage contribution of chondrocytes to bone cells is reduced (40%) in the deeper layers of the trabecular bone of the condylar neck; this region also correlates with relatively less *Adamts5* [5]. Collectively, the expression of *Adamts5*, reduction in bone density, and the developmental loss of

osteoblasts in *Adamts5*$^{-/-}$ mandibular condyles indicates that ADAMTS5 may play a role in the transdifferentiation of hypertrophic chondrocytes into osteoblasts in the mandibular condyle.

The specific function(s) of ADAMTS5 in bone formation within the mandibular condyle needs further experimentation. It has been well established that osteogenesis requires the expression of MMP9 and MMP13. Not only do ECM proteases cleave a variety of structural components of the ECM including native collagens, laminin, Acan and biglycan, but they also cleave non-ECM components and play a pivotal role in cell signaling cascades that are essential in mineralization during bone formation [25]. In this study we revealed that the localization of MMP13 was reduced in the mandibular condyles of *Adamts5*$^{-/-}$ mice potentially exacerbating the phenotype and loss of proteolytic activity of ECM substrates shared with ADAMTS5. The loss of MMP13 is likely due to the reduction of osteoblasts in the mandibular condyle of *Adamts5*$^{-/-}$ mice since osteoblasts express high levels of MMP13.

In the mandibular condyle of *Adamts5*$^{-/-}$ mice, there are also remnants of cartilage at the interface with bone. Since ADAMTS5 cleaves cartilage matrix components such as Acan, it may be required to degrade the structural matrix components of the hypertrophic chondrocytes which in turn signals dedifferentiation of hypertrophic chondrocytes. Studies have demonstrated that osteoprogenitors and osteoblasts secrete versican (Vcan) [26, 27] a substrate of ADAMTS5. In the present study, we showed that mesenchymal-like cells express *Vcan* in the transition zone of the mandibular condyle at early postnatal timepoints. Given that *Adamts5* was expressed predominantly by undifferentiated cells within the transition zone, cleavage of Vcan could induce differentiation of mesenchymal cells into osteoblasts (Figure 5). ADAMTS5 may also produce bioactive proteolytic fragments of its ECM substrates (Acan and Vcan) [18] [28], that facilitate bone formation.

Disruption of β-catenin signaling also interferes with the integration of chondrogenesis and osteogenesis in the mandibular condyle. Reduction of β-catenin resulted in greatly reduced transdifferentiation with a reduction in subchondral bone that coincided with reduced proliferation and differentiation in both chondrocytes and bone cells [29]. Abnormal upregulation of β-catenin in the MCC results in an increase in *Adamts5* expression [30]. Therefore, the results we observed in the *Adamts5*$^{-/-}$ mice are consistent with *Adamts5* expression being downstream in the Wnt, β-catenin pathway and involved in bone formation within the mandibular condyle.

Understanding the integration of cartilage degradation and bone formation is essential for implementation of regenerative medicine and for effective therapeutic targets that promote fibrocartilage and trabecular bone development. Although the involvement of ADAMTS5 in mandibular condylar development in large mammals needs to be investigated, the role of ADAMTS5 is likely conserved. Recent reports indicate that chondrogenesis and osteogenesis are a continuous process rather than two separate pathways [29]. While there is evidence that increased ADAMTS5 expression contributes to cartilage degeneration and disease progression of osteoarthritis, ADAMTS5 is also critical for the fibrocartilage [16] and trabeculated bone formation in development of the mandibular condylar. Future studies

will focus on the mandibular condylar degradome, the subset of the proteome encompassing proteases and their target ECM substrates that are integral to the coupling of mechanical force and bone formation in the mandibular condyle.

Supplementary Material

Refer to Web version on PubMed Central for supplementary material.

Acknowledgments:

The authors would like to acknowledge the histological expertise and contributions of Jeanette Huber, Emma Schafer and Ashton Lancaster.

1.9.9 **Role of funding sources:** American Heart Association #17GRNT33700214 (CBK), NIH, NHLBI HL121382 (CBK), T32 DE017551 (AWR, SCP), F30 1F30DEO28180 (AWR).

ABBREVIATIONS:

TMJ	Temporomandibular Joint
MCC	Mandibular condylar cartilage
ECM	extracellular matrix
ADAMTS5	A Disintegrin And Metalloproteinase with ThromboSpondin Motifs
MMP	Matrix Metalloproteinases
Acan	Aggrecan
Vcan	Versican
μCT	microcomputed tomography

1.9.11 References

1. Wang XD, Zhang JN, Gan YH, Zhou YH. Current understanding of pathogenesis and treatment of TMJ osteoarthritis. J Dent Res 2015; 94: 666–673. [PubMed: 25744069]
2. Milam SB. Pathogenesis of degenerative temporomandibular joint arthritides. Odontology 2005; 93: 7–15. [PubMed: 16170470]
3. Zhang J, Jiao K, Zhang M, Zhou T, Liu XD, Yu SB, et al. Occlusal effects on longitudinal bone alterations of the temporomandibular joint. J Dent Res 2013; 92: 253–259. [PubMed: 23340211]
4. Mizoguchi I, Toriya N, Nakao Y. Growth of the manddible and biological characteristics of the mandibular condylar cartilage. Japanese Dental Science Review 2013; 49: 139–150.
5. Hinton RJ, Jing Y, Jing J, Feng JQ. Roles of Chondrocytes in Endochondral Bone Formation and Fracture Repair. J Dent Res 2017; 96: 23–30. [PubMed: 27664203]
6. Chen W, Sun Y, Gu X, Hao Y, Liu X, Lin J, et al. Conditioned medium of mesenchymal stem cells delays osteoarthritis progression in a rat model by protecting subchondral bone, maintaining matrix homeostasis, and enhancing autophagy. J Tissue Eng Regen Med 2019; 13: 1618–1628. [PubMed: 31210406]
7. Kahn AJ, Simmons DJ. Chondrocyte-to-osteocyte transformation in grafts of perichondrium-free epiphyseal cartilage. Clin Orthop Relat Res 1977: 299–304.

8. Ono N, Ono W, Nagasawa T, Kronenberg HM. A subset of chondrogenic cells provides early mesenchymal progenitors in growing bones. Nat Cell Biol 2014; 16: 1157–1167. [PubMed: 25419849]
9. Yang G, Zhu L, Hou N, Lan Y, Wu XM, Zhou B, et al. Osteogenic fate of hypertrophic chondrocytes. Cell Res 2014; 24: 1266–1269. [PubMed: 25145361]
10. Yang L, Tsang KY, Tang HC, Chan D, Cheah KS. Hypertrophic chondrocytes can become osteoblasts and osteocytes in endochondral bone formation. Proc Natl Acad Sci U S A 2014; 111: 12097–12102. [PubMed: 25092332]
11. Jing Y, Zhou X, Han X, Jing J, von der Mark K, Wang J, et al. Chondrocytes Directly Transform into Bone Cells in Mandibular Condyle Growth. J Dent Res 2015; 94: 1668–1675. [PubMed: 26341973]
12. Kronenberg HM. Developmental regulation of the growth plate. Nature 2003; 423: 332–336. [PubMed: 12748651]
13. Mackie EJ, Tatarczuch L, Mirams M. The skeleton: a multi-functional complex organ: the growth plate chondrocyte and endochondral ossification. J Endocrinol 2011; 211: 109–121. [PubMed: 21642379]
14. Wylie JD, Ho JC, Singh S, McCulloch DR, Apte SS. Adamts5 (aggrecanase-2) is widely expressed in the mouse musculoskeletal system and is induced in specific regions of knee joint explants by inflammatory cytokines. J Orthop Res 2012; 30: 226–233. [PubMed: 21800360]
15. Botter SM, Glasson SS, Hopkins B, Clockaerts S, Weinans H, van Leeuwen JP, et al. ADAMTS5−/− mice have less subchondral bone changes after induction of osteoarthritis through surgical instability: implications for a link between cartilage and subchondral bone changes. Osteoarthritis Cartilage 2009; 17: 636–645. [PubMed: 19010693]
16. Rogers AW, Cisewski SE, Kern CB. The Zonal Architecture of the Mandibular Condyle Requires ADAMTS5. J Dent Res 2018; 97: 1383–1390. [PubMed: 29879379]
17. Jungers KA, Le Goff C, Somerville RP, Apte SS. Adamts9 is widely expressed during mouse embryo development. Gene Expr Patterns 2005; 5: 609–617. [PubMed: 15939373]
18. McCulloch DR, Nelson CM, Dixon LJ, Silver DL, Wylie JD, Lindner V, et al. ADAMTS metalloproteases generate active versican fragments that regulate interdigital web regression. Dev Cell 2009; 17: 687–698. [PubMed: 19922873]
19. Zhou X, von der Mark K, Henry S, Norton W, Adams H, de Crombrugghe B. Chondrocytes transdifferentiate into osteoblasts in endochondral bone during development, postnatal growth and fracture healing in mice. PLoS Genet 2014; 10: e1004820.
20. Ni W, Yang Z, Qi W, Cui C, Cui Y, Xuan Y. Gli1 is a potential cancer stem cell marker and predicts poor prognosis in ductal breast carcinoma. Hum Pathol 2017; 69: 38–45. [PubMed: 28965964]
21. Ishikawa Y, Nakatomi M, Ida-Yonemochi H, Ohshima H. Quiescent adult stem cells in murine teeth are regulated by Shh signaling. Cell Tissue Res 2017; 369: 497–512. [PubMed: 28547659]
22. Dupuis LE, McCulloch DR, McGarity JD, Bahan A, Wessels A, Weber D, et al. Altered versican cleavage in ADAMTS5 deficient mice; a novel etiology of myxomatous valve disease. Dev Biol 2011; 357: 152–164. [PubMed: 21749862]
23. Shi Y, He G, Lee WC, McKenzie JA, Silva MJ, Long F. Gli1 identifies osteogenic progenitors for bone formation and fracture repair. Nat Commun 2017; 8: 2043. [PubMed: 29230039]
24. Verma P, Dalal K. ADAMTS-4 and ADAMTS-5: key enzymes in osteoarthritis. J Cell Biochem 2011; 112: 3507–3514. [PubMed: 21815191]
25. Paiva KBS, Granjeiro JM. Matrix Metalloproteinases in Bone Resorption, Remodeling, and Repair. Prog Mol Biol Transl Sci 2017; 148: 203–303. [PubMed: 28662823]
26. Nakamura M, Sone S, Takahashi I, Mizoguchi I, Echigo S, Sasano Y. Expression of versican and ADAMTS1, 4, and 5 during bone development in the rat mandible and hind limb. J Histochem Cytochem 2005; 53: 1553–1562. [PubMed: 15983115]
27. Sanchez C, Mazzucchelli G, Lambert C, Comblain F, DePauw E, Henrotin Y. Comparison of secretome from osteoblasts derived from sclerotic versus non-sclerotic subchondral bone in OA: A pilot study. PLoS One 2018; 13: e0194591.

28. Lees S, Golub SB, Last K, Zeng W, Jackson DC, Sutton P, et al. Bioactivity in an Aggrecan 32-mer Fragment Is Mediated via Toll-like Receptor 2. Arthritis Rheumatol 2015; 67: 1240–1249. [PubMed: 25707860]

29. Jing Y, Jing J, Wang K, Chan K, Harris SE, Hinton RJ, et al. Vital Roles of beta-catenin in Trans-differentiation of Chondrocytes to Bone Cells. Int J Biol Sci 2018; 14: 1–9. [PubMed: 29483820]

30. Hui T, Zhou Y, Wang T, Li J, Zhang S, Liao L, et al. Activation of beta-catenin signaling in aggrecan-expressing cells in temporomandibular joint causes osteoarthritis-like defects. Int J Oral Sci 2018; 10: 13. [PubMed: 29686224]

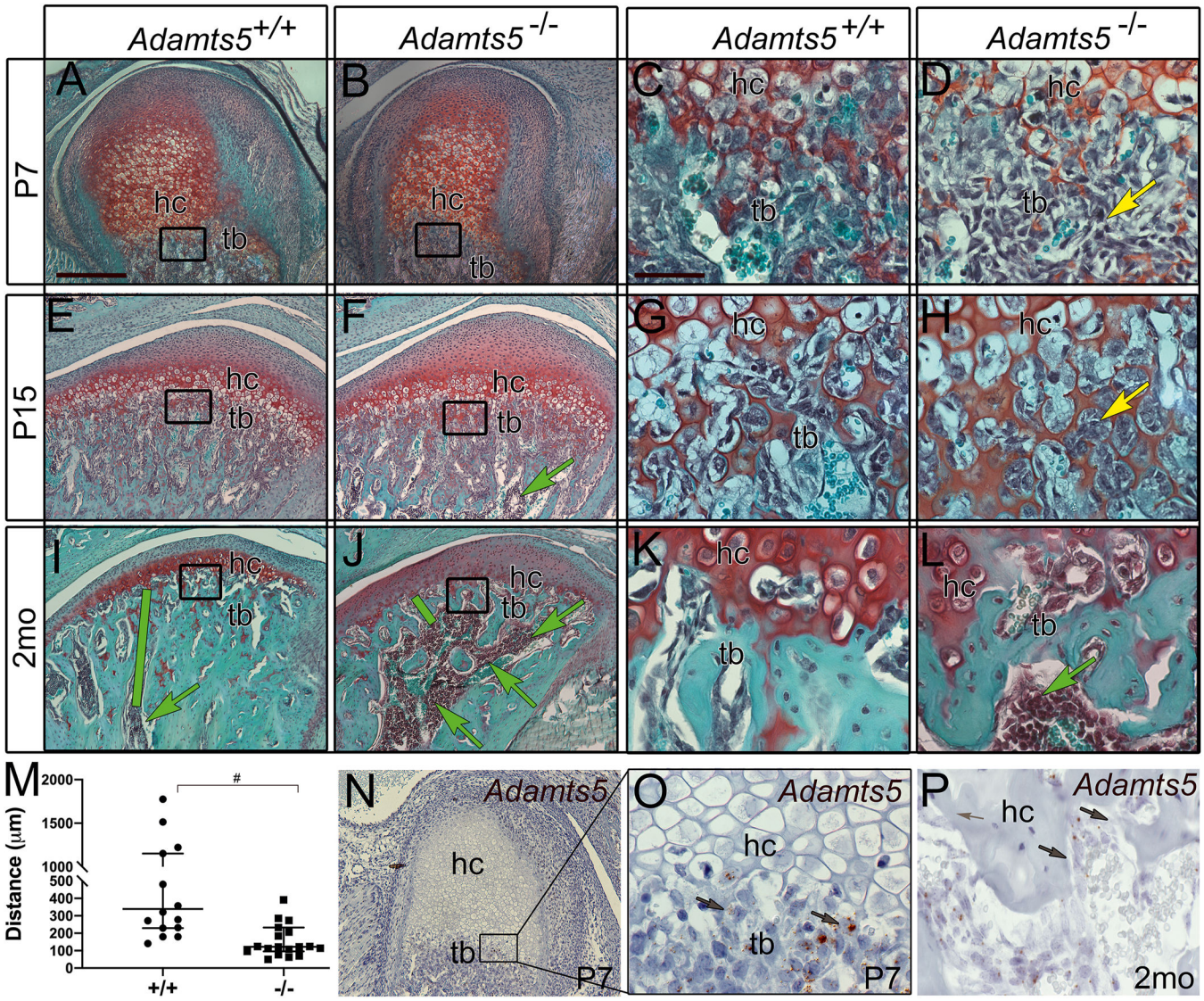

Figure 1: The interface of hypertrophic chondrocytes and trabeculated bone in the mandibular condyle is altered during development in *Adamts5*$^{-/-}$ mice and exhibits an increase in bone marrow.

Safranin O stained sections of the developing condyle at postnatal day 7 (P7) (A-D), P15 (E-H), and adult 2 month (2mo) (I-L), in *Adamts5*$^{+/+}$ (A, C, E, G, I, K, N-O) and *Adamts5*$^{-/-}$ (B, D, F, H, J, L). Cartilage bone interface region of hypertrophic chondrocytes (hc) and trabeculated bone (tb) (A, B, E, F, I, J black boxes magnified in C, D, G, H, K, L, respectively. Yellow arrow (D) indicates changes in mesenchymal cells in the transition zone of *Adamts5*$^{-/-}$ mandibular condyles (D, H). Green arrows (F, I, J, L) -bone marrow infiltration in the condylar head. Green bars (E, F) denote distance of bone marrow from the hc, graphed in I. Graph in M indicates the distance of the bone marrow from the transition zone containing the hypertrophic chondrocytes. Each point on the graph indicates data from one mouse. #- P<0.0001, Mann-Whitney U, 142; 95% CI −661.1 to −245.6, R= 0.2819. Expression of *Adamts5* using RNAscope™ (N-P, brown, arrows) at postnatal P7 (N, box in N magnified and shown in O). *Adamts5* expression in cells of the trabeculated bone in an

adult 2 month (2mo) (P, brown arrows) mandibular condyle. Bar in A = 200μm applies to B, E, F, I, J, N; bar in C = 50 μm applies to D, G, H, K, L, O, P.

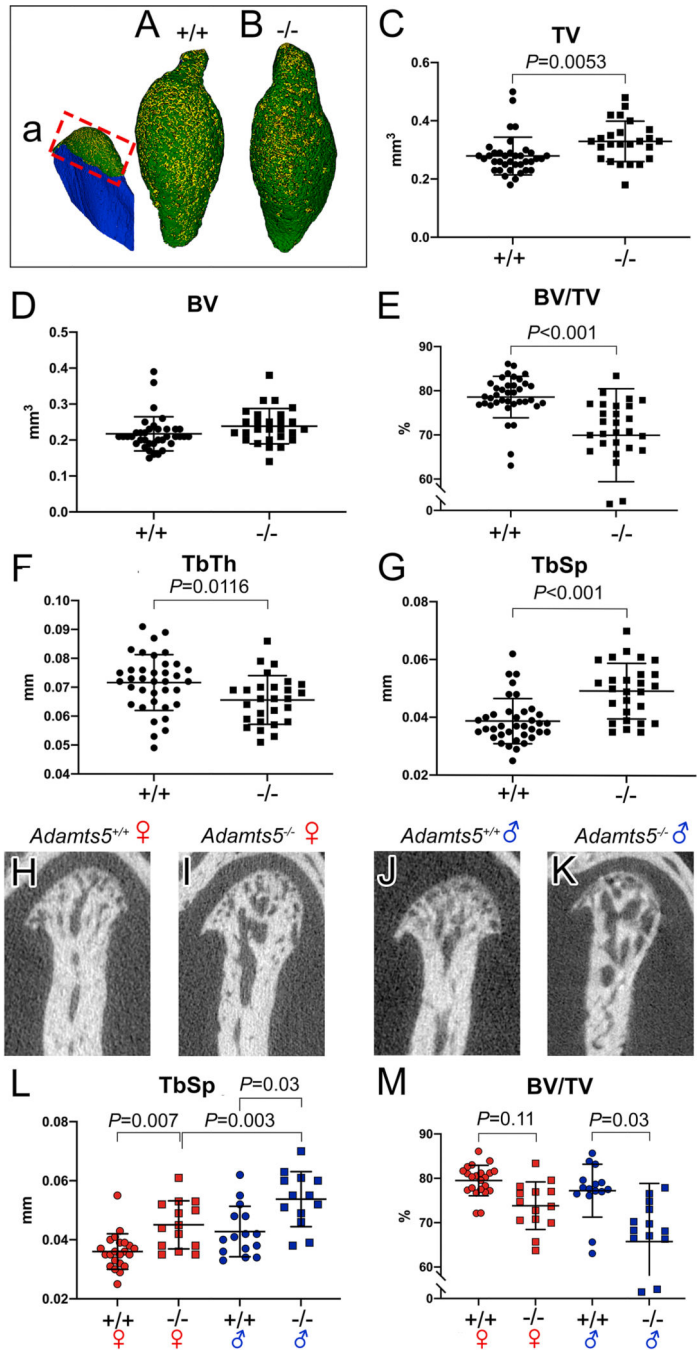

Figure 2: Young adult female and male *Adamts5*$^{-/-}$ mice exhibit changes in the subchondral bone of the mandibular condyle.

Three dimensional reconstructions of microtomography (μCT) of mandibular condyles in wild type (a, A) and *Adamts5*$^{-/-}$ mice (B). Red box in 'a' refers to the region of μCT analysis in C-M. Each point on the graph represents measurements from one condyle. TV-trabecular volume; BV-bone volume; BV/TV-bone volume/trabecular volume = bone density; Tb. Th-trabecular thickness; Tb. Sp. –trabecular spacing. H-K are two dimensional μCT slices of female *Adamts5*$^{+/+}$ (H), male *Adamts5*$^{+/+}$ (I), female *Adamts5*$^{-/-}$ (J) and male *Adamts5*$^{-/-}$ (K). μCT data was analyzed by sorting the sexes of mice (L, M), there was a

significant difference between male and female *Adamts5*$^{-/-}$ mice in the trabecular spacing of the mandibular condyle, and the bone density (BV/TV) was more significantly reduced in male mice compared to female mice. The longer bars on the graphs represent the average of the mean, with the shorter bars denoting standard deviation. Bar in C, P=0.0053; E, P<0.001; F, P=0.0116; G, P<0.001; L (left to right), P=0.007,P=0.003, P=0.03; M (left to right), P=0.11, 0.03.

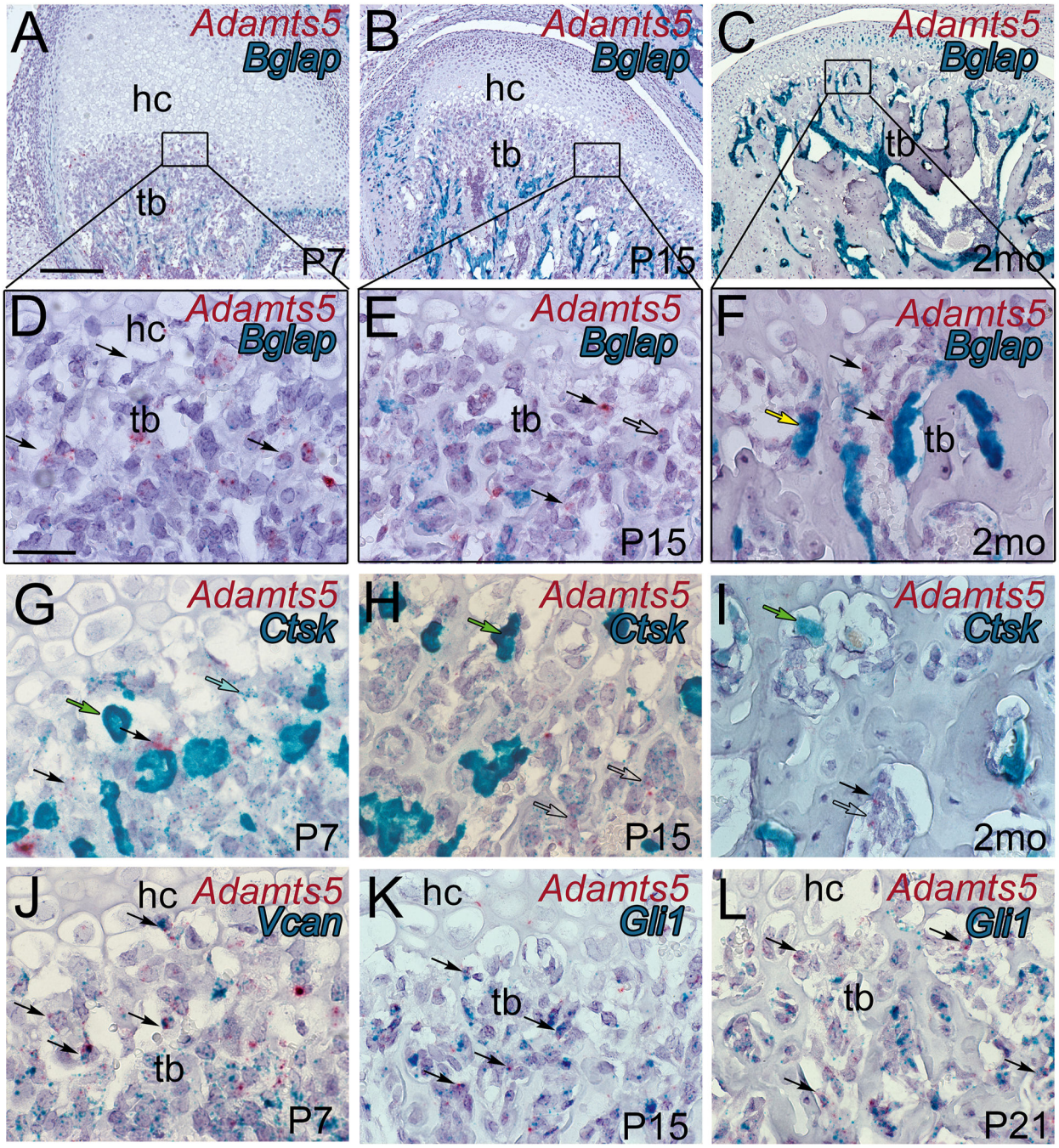

Figure 3: *Adamts5* expression overlaps with mesenchymal and stem cell markers in the trabeculated bone of the developing mandibular condyle.

Histological sections of the developing murine mandibular condyles *Adamts5* expression depicted in red (A-L) from a dual RNAscope™ assay with bone gamma-carboxyglutamic acid-containing protein (*Bglap*) (A-F, blue-green), Cathepsin K (*Ctsk*) (G-I, blue-green), versican (Vcan) (J, blue-green) and glioma associated oncogene 1 (*Gli1*) (K, L, blue-green). Postnatal day 7 (P7); Postnatal day 15 (P15); postnatal day 21 (P21); hc-hypertrophic chondrocytes; tb-trabeculated bone; black arrows in A-L-*Adamts5* (red) expressing cells; open arrow in E, colocalization of *Adamts5* and *Bglap*; yellow arrow-differentiated

osteoblast; green arrows-osteoclasts; blue arrow-low expressing *Cstk* cell co-expressed with *Adamts5*; open arrows in H, I, -low level expressing *Cstk* cells with co-expression of *Adamts5*; black arrows in J -co-expression of *Vcan* and *Adamts5*; black arrows in K, L -co-expression of *Gli1* and *Adamts5*. Bar in A = 200 μm applies to B, C; bar in D = 50 μm applies to E-L.

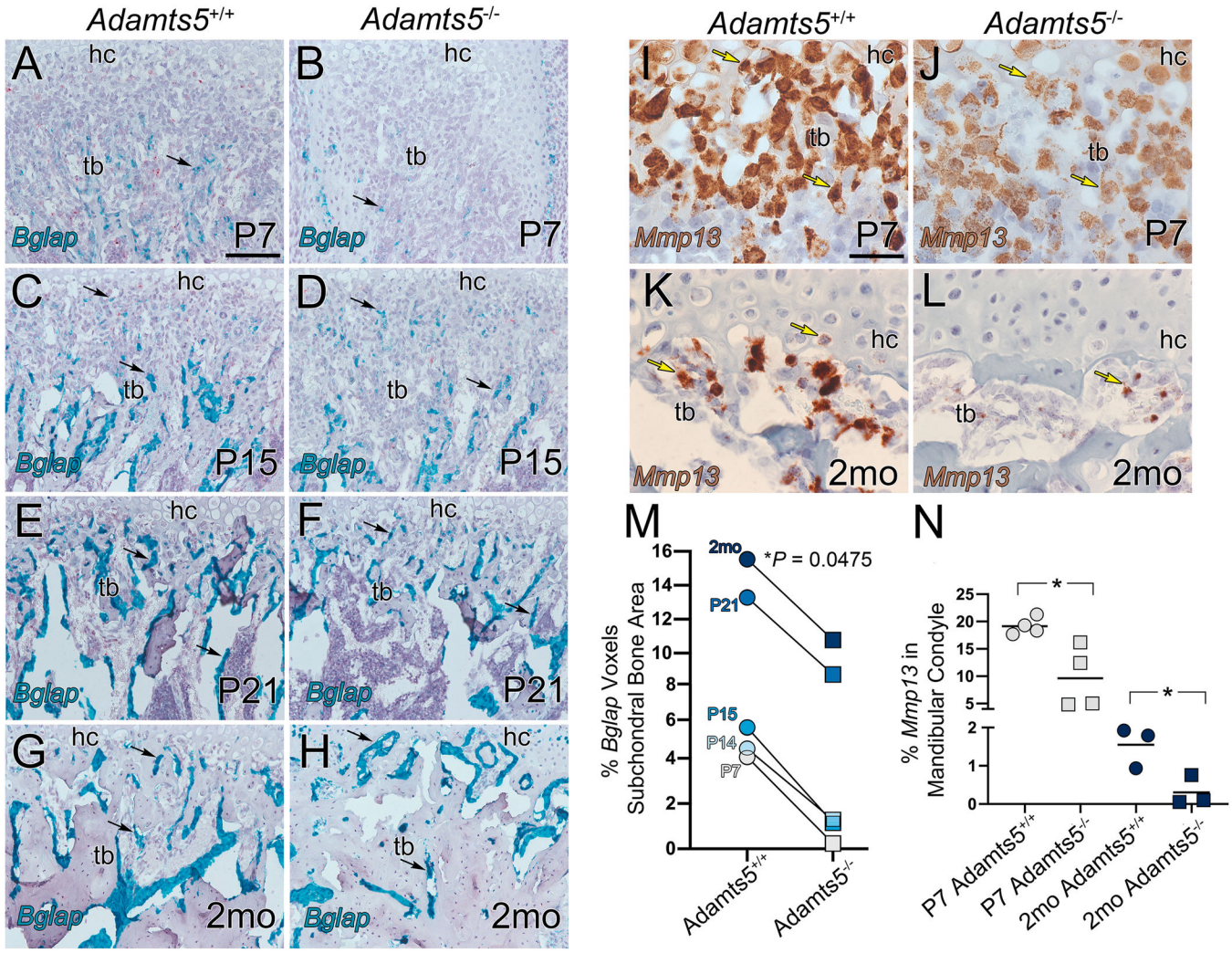

Figure 4: There is a reduction of osteoblast marker *Bglap* and MMP13 expression in the transition zone of the *Adamts5* deficient mandibular condyles.

Bglap (osteocalcin precursor) expression was evaluated in the developing mandibular condylar bone of wildtype and *Adamts5* deficient mice at P7, P14, P15, P21, and 2mo (A-H, blue-green). At each developmental stage there was significantly more *Bglap* expression in the wildtype condyles than Adamts5 deficient shown quantified in the graph (M). The grey lines in M are drawn from the wildtype and *Adamts5* deficient values to highlight the age-matched reduction of Bglap expression in the *Adamts5* deficient condyle; 95%CI 0.07840 to 0.9773. *Mmp13* expression was also evaluated at P7 and 2mo (I-L), at each stage there was a significant reduction in MMP13 expression in the *Adamts5* deficient mandibular condyles compared to wildtype (N). In graphs circles depict wildtype and squares indicate *Adamts5* deficient values. Each symbol on the graph represents measurements from one condyle. Black arrows in A-H-expression of *Bglap*; yellow arrows in I-L-expression of *Mmp13*. Bar in A = 100 μm applies to B-H; bar in I = 50 μm applies to J-L. Bglap 95%CI 0.07840 to 0.9773; Mmp13, P7, 95%CI −16.68 to −2.373; Mmp13, 2mo, 95%CI −2.314 to −0.1828.

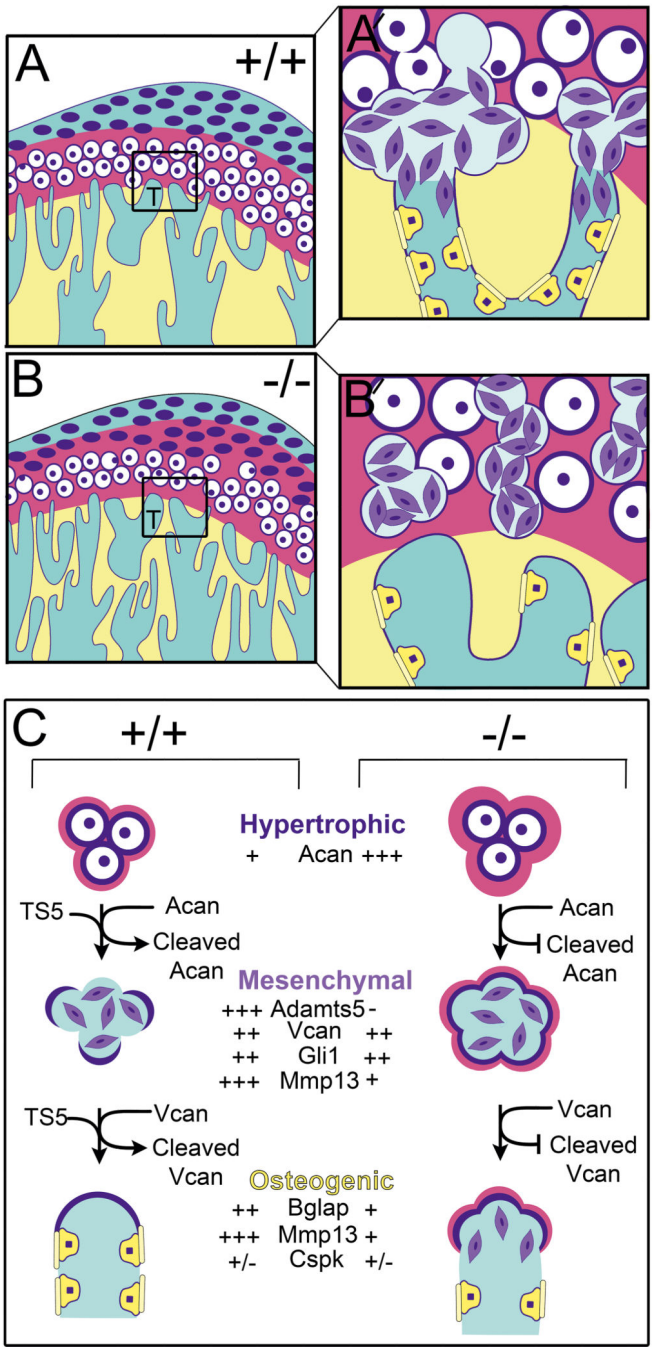

Figure 5. Schematic model depicting a role for ADAMTS5 in the developing trabeculated bone of the mandibular condyle.

At the cartilage bone interface (transition zone) in the developing mandibular condyle hypertrophic cells undergo ‘transdifferentiation’ into bone-producing cells, a process that is poorly understood but that we reveal a role for ADAMTS5. In mice devoid of *Adamts5* there is a reduction of trabeculated bone in the mandibular condyle and less bone-forming cells during postnatal development. *Adamts5* is expressed by stem cell-like mesenchymal cell progenitors (purple cells) that are derived from hypertrophic chondrocytes at the cartilage-bone interface in the condylar head (boxes in A, B, in high magnification in

A′ and B′). Mesenchymal cells in this transition zone also express *Vcan*, a proteoglycan substrate of ADAMTS5; VCAN cleavage in other contexts facilitates differentiation and reduces proliferation. ADAMTS5 generated by the mesenchymal cells degrades the ACAN-rich cartilage matrix and pericellular ECM of hypertrophic chondrocytes (magenta) at the transition zone. Once this cartilage ECM is degraded and the pericellular matrix shell of the hypertrophic chondrocytes is partially removed, fusion occurs with blood vessels at the interface with the trabeculated bone. Next the mesenchymal cells appear to migrate into and adhere to the vessel walls, differentiate into osteoblast-like cells (yellow cells) and deposit osteoid (yellow bars) on the endosteal surface of bone (yellow). Fully differentiated osteoblasts (*Bglap* expressing) do not express detectable levels of *Adamts5* indicating a transient role for this protease in the stem-like mesenchymal cell stages. The reduction of *Mmp13* in *Adamts5* deficient condyles likely contributes to the bone phenotype since *Mmp13* is a key factor in bone mineralization.